NB-GTR: Narrow-Band Guided Turbulence Removal

Supplementary Material

Yifei Xia[1,2] Chu Zhou[3] Chengxuan Zhu[3] Minggui Teng[1,2] Chao Xu[3] Boxin Shi*[1,2]

[1] National Key Laboratory for Multimedia Information Processing, School of Computer Science, Peking University

[2] National Engineering Research Center of Visual Technology, School of Computer Science, Peking University

[3] National Key Lab of General AI, School of Intelligence Science and Technology, Peking University

{yfxia, zhou_chu, peterzhu, minggui_teng, shiboxin}@pku.edu.cn, xuchao@cis.pku.edu.cn

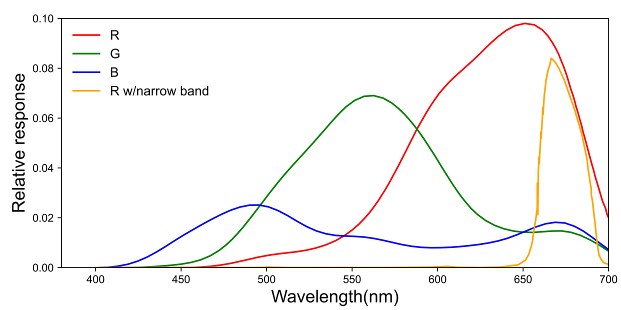

Figure 7. camera response curve [2]

6. Details of narrow-band imaging

Corresponding to Footnote 1 in Section 3.1 of the main paper, Figure 7 displays the typical response curves of R, G, B filters of a CMOS [2]. The narrow-band filter used in our experiment has a central wavelength of $\lambda_0 = 680\,\text{nm}$, a bandwidth of $\Delta\lambda = 40\,\text{nm}$, and a response curve of $f(\lambda)$. The combination of the broad-band R filter and the narrow-band filter results in a narrower response curve, labeled as *R w/narrow band* in Figure 7, which reduces total variance and produces a less turbulent observation.

7. Details of Turbulence Synthesis

In this section, we present further details of the paired turbulence synthesis, which simulates a simultaneously captured RGB and narrow-band turbulent image pair from a single clear i mage.

RGB image. To synthesize an RGB turbulent image, we first established the physical parameters for images captured through atmospheric turbulence. These settings broadly follow the configuration in [6], covering common atmospheric turbulence strengths and camera settings, as shown in Table 3. After synthesizing the turbulence, we added noise to the images. Gaussian noise was introduced with a standard deviation in the range of 0.005 to 0.015 for RGB images.

Table 3. Parameters for turbulence simulation. The notation $[\cdot,\cdot]$ is used to indicate uniform sampling on a continuous interval, while $\{\}$ is used to denote uniform sampling on a set of discrete values.

D/r_0	Distance (m)	Focal length (m)	F-number
[0.75, 5.25]	[200, 400]	[1, 2]	{8, 11}
			{5.6, 8, 11}
	[400, 600]	[1, 2.5]	{8, 11, 16}
			{5.6, 8, 11}
	[600, 800]	[1, 3]	{11, 16}
			{8, 11}

Narrow-band image. We modified the physical parameters and the Zernike scaler inside the P2S simulator [8] to synthesize a narrow-band image taken at the same time as the RGB image. This was done by taking into account the dependence of atmospheric turbulence on wavelength. We adjusted both the wavelength and the Fried parameter [4] for the narrow-band images. According to [5], the Fried parameter $r_0(\lambda_2)$ of the narrow-band image can be calculated from the Fried parameter $r_0(\lambda_1)$ of the RGB image at the same moment using the following formula:

$$r_0(\lambda_2) = \left(\frac{N(\lambda_1)\lambda_2}{N(\lambda_2)\lambda_1}\right)^{6/5} r_0(\lambda_1), \tag{1}$$

where N is defined by Equation 1 in the main paper. Given that the P2S simulator [8] is based on Zernike polynomials, we also adjusted each Zernike coefficient according to the relationship between the Zernike coefficients and the wavelength, as measured in [10]. The new coefficients are approximately inversely proportional to the wavelength, as follows:

$$a_j(\lambda_2) = \frac{\lambda_1}{\lambda_2} a_j(\lambda_1), \tag{2}$$

where a_j is the j-th Zernike coefficient defined in [8].

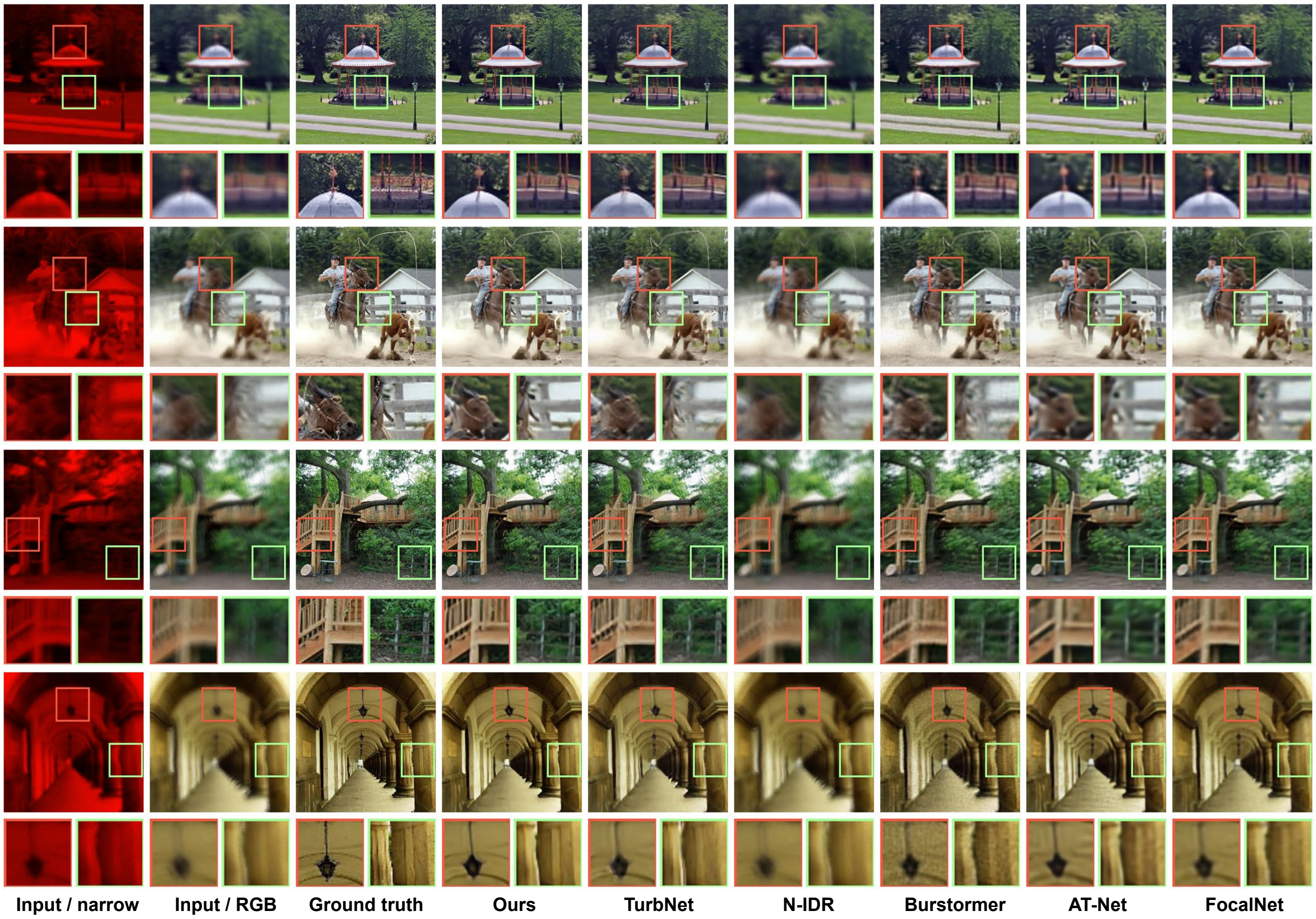

Figure 8. Additional visual comparison on synthetic dataset.

Table 4. Quantitative comparison under three different turbulence strengths, with three turbulence removal methods N-IDR [7], AT-Net [11], TurbNet [9] and two general image restoration methods Burstormer [3], FocalNet [1] on synthetic data. All compared methods are retrained given a pair of RGB and narrow-band images.

Methods	Weak		Medium		Strong	
	PSNR	SSIM	PSNR	SSIM	PSNR	SSIM
N-IDR [7]	22.22	0.6760	20.46	0.5615	19.43	0.4906
Burstormer [3]	22.68	0.7057	21.21	0.6163	20.17	0.5460
AT-Net [11]	22.81	0.7212	22.21	0.6906	21.48	0.6500
FocalNet [1]	24.52	0.8010	22.54	0.7062	21.30	0.6341
TurbNet [9]	24.94	0.8311	22.88	0.7396	21.67	0.6762
NB-GTR	**26.93**	**0.8839**	**24.71**	**0.8151**	**23.31**	**0.7589**

After the turbulence simulation, we adjusted the RGB channels of the narrow-band image by giving them coefficients of 0.95, 0.04, and 0.01, respectively. This adjustment was done to make the simulation results match the average distribution that was determined through actual narrow-band photography. Lastly, Gaussian noise was added to the images, with a standard deviation ranging from 0.015 to 0.025 for narrow-band images, to create a noisier image than the RGB image.

8. Additional Experimental Results

In this section, we provide more visual comparison of our NB-GTR with three turbulence removal methods N-IDR [7], AT-Net [11], TurbNet [9] and two general image restoration methods Burstormer [3], FocalNet [1], as is shown in Figure 8. We conducted further research to determine the effect of turbulence strength on the efficacy of turbulence removal methods on our synthetic dataset. The results are shown in Table 4, where the turbulence strength is divided into three categories based on the values of D/r_0: $0.75 - 2.25$ for *weak*, $2.25 - 3.75$ for *medium*, and $3.75 - 5.25$ for *strong* perturbations. Our method proved to be more effective than the other approaches.

References

[1] Yuning Cui, Wenqi Ren, Xiaochun Cao, and Alois Knoll. Focal network for image restoration. In *Proc. of International Conference on Computer Vision*, 2023. 2

[2] Jason Deglint, Farnoud Kazemzadeh, Daniel Cho, David A Clausi, and Alexander Wong. Numerical demultiplexing of color image sensor measurements via non-linear random forest modeling. *Scientific reports*, 6(1):28665, 2016. 1

[3] Akshay Dudhane, Syed Waqas Zamir, Salman Khan, Fahad Shahbaz Khan, and Ming-Hsuan Yang. Burstormer: Burst image restoration and enhancement Transformer. *arXiv preprint arXiv:2304.01194*, 2023. 2

[4] David L Fried. Optical resolution through a randomly inhomogeneous medium for very long and very short exposures. *Journal of the Optical Society of America*, 56(10): 1372–1379, 1966. 1

[5] Russell C Hardie, Michael A Rucci, Santasri Bose-Pillai, Richard Van Hook, and Barry K Karch. Modeling and simulation of multispectral imaging through anisoplanatic atmospheric optical turbulence. *Optical Engineering*, 61(9): 093102–093102, 2022. 1

[6] Ajay Jaiswal, Xingguang Zhang, Stanley H Chan, and Zhangyang Wang. Physics-driven turbulence image restoration with stochastic refinement. In *Proc. of International Conference on Computer Vision*, 2023. 1

[7] Nianyi Li, Simron Thapa, Cameron Whyte, Albert W Reed, Suren Jayasuriya, and Jinwei Ye. Unsupervised non-rigid image distortion removal via grid deformation. In *Proc. of International Conference on Computer Vision*, 2021. 2

[8] Zhiyuan Mao, Nicholas Chimitt, and Stanley H Chan. Accelerating atmospheric turbulence simulation via learned phase-to-space transform. In *Proc. of International Conference on Computer Vision*, 2021. 1

[9] Zhiyuan Mao, Ajay Jaiswal, Zhangyang Wang, and Stanley H Chan. Single frame atmospheric turbulence mitigation: A benchmark study and a new physics-inspired Transformer model. In *Proc. of European Conference on Computer Vision*, 2022. 2

[10] Fang Wang, Qiyuan Zhang, Haoyu Wang, Dayong Zhu, Huaikang Zhu, Wenxin Jia, and Sen Han. An improved fitting method for predicting the zernike coefficient–wavelength curves. *IEEE Photonics Journal*, 13(2):1–17, 2021. 1

[11] Rajeev Yasarla and Vishal M Patel. Learning to restore images degraded by atmospheric turbulence using uncertainty. In *Proc. of International Conference on Image Processing*, 2021. 2